

000 001 JACKPOT: ALIGN ACTOR-POLICY DISTRIBUTION FOR 002 SCALABLE AND STABLE RL FOR LLM 003 004

005 **Anonymous authors**

006 Paper under double-blind review

007 008 ABSTRACT 009

011 Reinforcement learning (RL) has become an increasingly important paradigm for
012 improving large language models (LLMs) on alignment, reasoning, and coding tasks,
013 yet it remains extremely costly. The majority of training time is spent on rollouts.
014 Allowing actor and policy distributions to differ could unlock substantial scalability and
015 efficiency benefits, such as supporting large-batch or asynchronous training, and even
016 enabling a lightweight rollout model. However, existing importance sampling-based
017 corrections for distribution mismatch suffer from an inherent trade-off between stability
018 and training performance. To tackle this problem, we propose Jackpot, which leverages
019 Optimal Budget Rejection Sampling to directly reduce the gap between actor and policy
020 distributions. For efficiency and stability in practical training, We introduce an efficient
021 probability estimation strategy based on Top- K logits with batch bias correction, and
022 designs a stabilized Jackpot-PPO loss that jointly accounts for both the importance
023 sampling ratio and the trust-region constraint in PPO. Empirically, our method achieves
024 stable improvements in large-batch and asynchronous training, and in extreme off-policy
025 training it substantially delays the onset of collapse and delivers competitive performance.
026 Specifically, we achieve 20% improvement on AMC benchmarks and 8% AIME
027 benchmarks over the off-policy baseline under 128 \times actor-policy update ratio for
028 Qwen3-4B-Base and 64 \times for Qwen3-8B-Base, while achieving greater stability and
029 better performance than prior off-policy RL methods under extreme settings.

030 1 INTRODUCTION 031

032 Reinforcement learning (RL) has demonstrated substantial effectiveness in the post-training of large language
033 models (LLMs), yielding significant improvements in domains such as mathematics (Guo et al., 2025;
034 Azerbayev et al., 2023), coding (Jimenez et al., 2023; Ouyang et al., 2025), and agentic tasks (Liu et al., 2023).
035 Despite these successes, RL remains computationally expensive (Sheng et al., 2025; Fu et al., 2025; Zheng
036 et al., 2025b), with the majority of the training cost, often exceeding 70%, attributed to rollouts, wherein
037 LLMs generate solution trajectories for tasks in order to compute rewards. If actors and policies were allowed
038 to follow different distributions, the scalability and efficiency of RL could be elevated to an entirely new level.
039 For instance, such flexibility would make it possible to support large-batch or asynchronous training, thereby
040 improving the utilization of serving systems (Zheng et al., 2025a). Moreover, quantized or sparse models,
041 and even distilled smaller models, could be deployed as actors to further enhance efficiency. In practice,
042 however, the mismatch between actor and policy distributions often leads to instability and severe degradation
043 in performance (Liu et al., 2025), posing a fundamental barrier to the reliable adoption of these techniques.

044 When the distribution gap between the actor and the policy becomes large, existing importance sampling
045 (IS)-based correction methods (Liu et al., 2025; Wu et al., 2025b; Fu et al., 2025) perform suboptimally
046 compared with the baseline PPO. In practice, truncated importance sampling methods (TIS) either
047 underperform or exhibit substantial convergence gap to the on-policy baseline when the truncation threshold
048 is low or conservative, or TIS crashes before policy plateaus from RL training when the truncation threshold
049 is set to a higher or aggressive value. The importance weight used by TIS is $\frac{p_{\text{ref}}(a)}{p_{\text{target}}(a)}$. Once the actor
050 drifts too far, many tokens that the actor samples with high probability have very low probability under
051 the policy, since $p_{\text{inf}} > p_{\text{target}}$. These actor trajectories are effectively treated as low-likelihood samples by
052 the policy, causing TIS to train on tokens the policy would never select at inference and creating a widening
053 train-inference mismatch. This naturally raises the following question: *Can we directly modify the actor's
sampling distribution and sampled trajectories to reduce its distributional gap to the policy?*

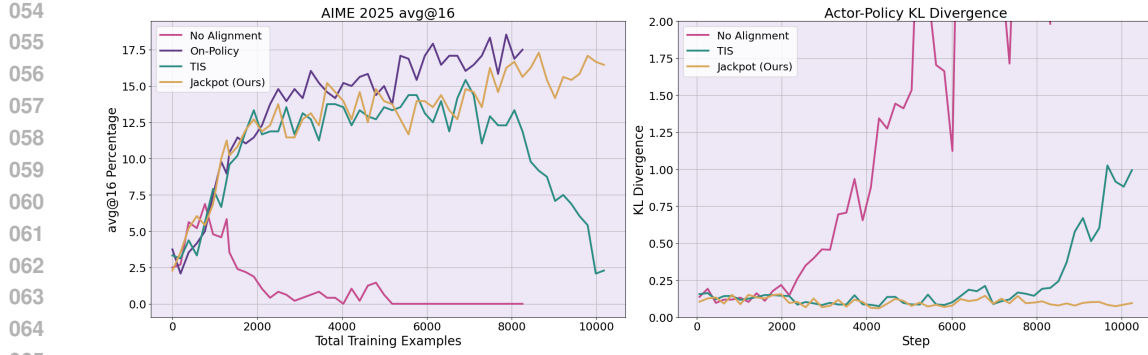


Figure 1: RL training requires actor-policy maintaining strong probability distribution alignment. When actor and policy aren't aligned, they will result in training collapse. Here we show training setting use a Qwen3-1.7B-Base model training rollout to train a Qwen3-8B-Base model policy. Without any alignment procedures, training collapses (pink). Prior method TIS (green) also show significant gap towards Qwen3-8B-Base on-policy baseline (purple), while collapsing, using TIS sees KL divergence also violently increasing. Our proposed method, Jackpot (yellow) maintains small KL divergence between actor and policy model probability distribution, while showing stable and competitive training convergence to on-policy setting.

Rejection sampling, which can simulate a target distribution from an accessible proposal distribution, has a long history and has been widely applied in fields such as biology (Carrella et al., 2024), the social sciences, machine learning (Naesseth et al., 2016), and statistics (Martino & Míguez, 2011; Gilks et al., 1995). However, a direct application of rejection sampling is prohibitively expensive in the context of RL. Specifically, token i must be accepted with probability $\frac{p_i}{\lambda q_i}$, where $\lambda = \max_i \frac{p_i}{q_i}$. For contemporary LLMs, which typically possess vocabularies exceeding 100,000 tokens, this constant C can become extremely large, since the majority of token probabilities are exceedingly close to zero. As a result, nearly all tokens proposed by the actor are rejected, rendering naive rejection sampling impractical for large-scale RL and leading to prohibitively low sample efficiency. Fortunately, Optimal Budget Rejection Sampling (OBRS) (Verine et al., 2024) relaxes the requirement of classical rejection sampling and, although it does not enforce the actor distribution to be identical to the policy distribution, it provably reduces their distance and guarantees that for any rejection ratio the adjusted actor distribution is strictly closer to the policy distribution than the unadjusted one. This provides us with an opportunity fundamentally different from standard rejection sampling.

However, applying OBRS directly in RL systems introduces several technical challenges. First, PPO relies on the existence of a trust region to stabilize the training process, which means that modifying the actor probabilities through OBRS may compromise training stability. Second, in order to compute the true probabilities of the remaining tokens after the rejection process, OBRS requires access to the probabilities of all tokens in the vocabulary, which imposes significant memory overhead for modern LLMs with extremely large vocabularies.

In this paper, we propose JACKPOT, which consists of three key components. First, an OBRS-based masking mechanism ensures that the adjusted actor distribution remains strictly closer to the policy distribution. Second, an efficient probability estimation strategy is introduced, which leverages Top- K logits together with batch-wise bias correction to approximate the full-vocabulary probabilities while mitigating memory overhead. Third, we design a stabilized JACKPOT-PPO loss that jointly accounts for both the importance sampling ratio and the trust region constraint in PPO, thereby preserving training stability.

To validate the effectiveness of our method, we consider two representative scenarios. **(1) Large-batch training.** In this setting, the LLM generates up to 128 mini-batches in a single rollout step, which enables more efficient utilization of serving system hardware resources. Empirically, we observe more than a $2\times$ improvement in end-to-end RL throughput compared to on-policy training. However, this comes at the cost of substantial policy drift during training, resulting in significant divergence between the rollout actor and the updated policy. **(2) Extreme off-policy training.** In this setting, we employ a fixed model for rollouts that is different from the one being optimized. This configuration introduces a severe distributional mismatch, under which standard approaches typically fail and training collapses rapidly.

We organize the remainder of this paper as follows.

- In Section 2, we formally introduce the distribution mismatch between actors and policy, discuss its sources under different training scenarios, and review related work.
- In Section 3, we describe our application of OBRs to RL and validate its effectiveness through numerical experiments and empirical observations.
- In Section 4, we provide a detailed description of JACKPOT-PPO, including three key components: (i) OBRs masking, (ii) efficient probability estimation with Top- K logits and batch bias correction, and (iii) a stabilized JACKPOT-PPO loss that jointly considers importance sampling ratios and PPO’s trust-region constraint.
- In Section 5, we present experiments on Qwen models and mathematical reasoning tasks to validate JACKPOT. First, in large-batch training, our method maintains stable learning, outperforming offline and TIS baselines and approaching the performance of the online setting. Second, in extreme off-policy training, the proposed method substantially delays the onset of training collapse and achieves competitive performance.

Using JACKPOT, we achieve 20% improvement on AMC benchmarks and 8% AIME benchmarks over the off-policy baseline under $128\times$ actor-policy update ratio for Qwen3-4B-Base and $64\times$ for Qwen3-8B-Base, while achieving greater stability and better performance than prior off-policy RL methods under extreme settings. Overall, JACKPOT is simple to plug in, theoretically well-grounded, and holds the potential to enable more aggressive forms of off-policy RL.

2 BACKGROUND

In this section, we first formalize the distribution mismatch problem that arises in RL for LLMs. We then review several strands of related work of JACKPOT.

2.1 PROBLEM SETTING: PPO OBJECTIVE AND ACTOR-POLICY DISTRIBUTION MISMATCH

We begin with the clipped objective in PPO (Schulman et al., 2017), whose expectation can be written as

$$\mathcal{L}^{\text{PPO}}(\theta) = \mathbb{E}_{x \sim P_{\text{inf}}} \left[\min \left(r_{\theta}(x) \hat{A}(x), \text{clip} \left(r_{\theta}(x), 1 - \epsilon, 1 + \epsilon \right) \hat{A}(x) \right) \right] \quad (1)$$

where $r_{\theta}(x) = p_{\theta_{\text{new}}}(x)/p_{\text{ref}}(x)$ is the likelihood ratio between the updated policy $p_{\theta_{\text{new}}}$ and the reference policy p_{ref} , and $\hat{A}(x)$ denotes the estimated advantage at decision x . p_{inf} is the inference distribution used to generate rollouts, p_{ref} is the reference policy distribution assumed in the objective, and $p_{\theta_{\text{new}}}$ is the updated policy distribution. In the standard process, it is assumed that $p_{\text{inf}} = p_{\text{ref}}$, but in practice this assumption is often violated, leading to actor–policy distribution mismatch.

Distribution mismatch is common and arises for several reasons, such as minor discrepancies between the inference engine and the reference policy by FSDP engines, the use of stale or asynchronous data, or rollouts generated by approximated models (e.g., quantized, sparsified, or distilled). Such mismatches can destabilize training and therefore require additional mechanisms to correct or mitigate their impact. .

2.2 RELATED WORK

RL for LLM. Reinforcement learning has been widely applied to LLMs to improve human alignment, reasoning, coding, and other complex tasks. Beyond PPO, memory efficient methods have been proposed, including ReMax (Li et al., 2023), RLOO (Ahmadian et al., 2024), and GRPO (Shao et al., 2024). In addition, methods such as SimPO (Meng et al., 2024) and DPO (Rafailov et al., 2023), which are based on offline RL, have also been employed for human alignment. RL training systems for LLMs, such as Verl (Sheng et al., 2025), AReal (Fu et al., 2025), TRL (von Werra et al., 2020), and OpenRLHF (Hu et al., 2024), have been developed to improve training throughput and scalability.

Distribution Mismatch Correction in RL. Actor-policy mismatch is a common problem that has long been studied, e.g. Impala Espeholt et al. (2018). To alleviate the actor-policy distribution gap, the method introduces a truncated importance sampling (TIS) to approximate the true PPO objective.

$$\mathcal{L}^{\text{PPO}}(\theta) = \mathbb{E}_{x \sim P_{\text{inf}}} \left[\min \left(\frac{p_{\text{ref}}(x)}{p_{\text{inf}}(x)}, C \right) \min \left(r_{\theta}(x) \hat{A}(x), \text{clip} \left(r_{\theta}(x), 1 - \epsilon, 1 + \epsilon \right) \hat{A}(x) \right) \right] \quad (2)$$

The truncation threshold C is for maintaining the stability of the range of the importance ratio. Recently, several methods apply the truncated importance sampling method to RL of LLMs. Methods such as FlashRL (Liu et al., 2025), AReal (Fu et al., 2025), and LlamaRL (Wu et al., 2025b) address distribution mismatch by introducing (truncated) importance sampling ratios, typically of the form $p_{\text{ref}}/p_{\text{inf}}$, to correct the impact of mismatch on

162 advantage estimation. From system perspective, FP32 LM heads (Liu et al., 2025) and deterministic LLM
 163 Inference (He & Lab, 2025) are implemented to mitigate the numerical issue of serving systems when rollout.
 164

165 In this paper, we proposed JACKPOT. Our method is **orthogonal** to the above prior works. We directly modify
 166 p_{inf} through rejection sampling and reweighting of the output probabilities so that the divergence between p_{inf}
 167 and the target distributions p_{ref} is provably reduced. Moreover, techniques such as TIS can be applied on top
 168 of this improved distribution to further correct the remaining mismatch in a complementary way. JACKPOT
 169 offers a mechanism that is shown to be effective in stabilizing RL training under severe mismatches.

170 3 CORRECTING DISTRIBUTION MISMATCH WITH BUDGETED REJECTION SAMPLING

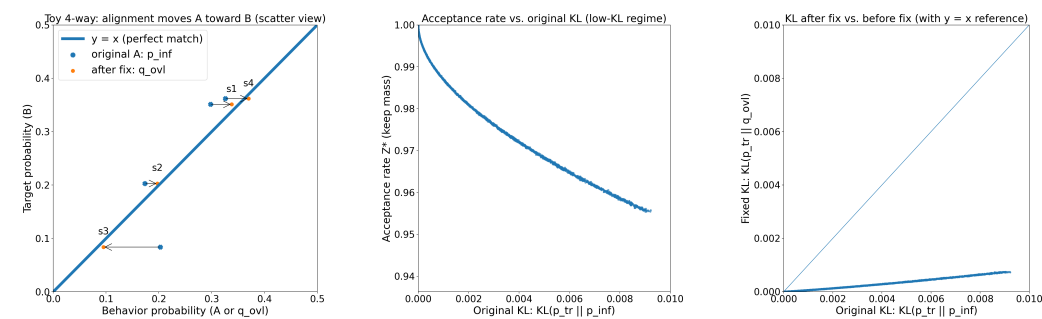
173 One of the most fundamental challenges of modern RL framework for LLMs is the distributional mismatch
 174 between samples generated by our inference model (actor), or p_{inf} , and the true reference policy distribution,
 175 or $p_{\theta_{\text{ref}}}$. One way is through Importance Sampling, or adding an importance ratio term $\frac{p_{\text{ref}}}{p_{\text{inf}}}$. However, as the
 176 trajectories are sampled and $p_{\text{inf}}(x)$ can be small, the importance ratio sometimes blows up in numeric value.
 177 In practice, $\min(\frac{p_{\text{ref}}}{p_{\text{inf}}}, C)$ is used Espeholt et al. (2018) to cap out the dangerously large values, leading to huge
 178 bias in correcting the distribution misalignment. Instead of solely relying on Importance Sampling, can we
 179 modify p_{inf} and the sampled trajectories directly so that it is closer in probability distribution to p_{ref} ?

180 One direct idea is **Rejection Sampling (RS)**, or stochastically rejecting tokens in the tractoryes sampled with
 181 p_{inf} based on the difference between the two distributions. Once a token is rejected, it contributes nothing
 182 to the loss and gradient calculation. While canonical rejection sampling could resolve this, its application
 183 here—using p_{inf} as the proposal and $p_{\theta_{\text{new}}}$ as the target—is impractical, as rejection sampling aims for
 184 identical probability distribution after correction. The potentially large divergence between these distributions
 185 would lead to a prohibitively low acceptance rate, essentially leading to most tokens being rejected. The
 186 data efficiency of RL training will be severely degraded, failing to meet practical requirements.

187 To overcome this, we adopt the principled approach of **Optimal Budgeted Rejection Sampling (OBRS)**
 188 (Verine et al., 2024). This technique reframes the problem: instead of demanding perfect adherence to the
 189 target distribution at the cost of sample efficiency, it seeks the optimal rejection rule that, for a given target
 190 acceptance rate (a “budget”), produces a distribution as close as possible to the target. This is precisely the
 191 trade-off our problem requires.

192 The method employs a scaled acceptance probability, where a scaling factor λ is chosen to meet the desired
 193 sample throughput. A token a sampled from the proposal p_{inf} is accepted with probability $\alpha_C(a)$ defined
 194 as $\alpha_C(a) = \min\left(1, \frac{p_{\text{target}}(a)}{\lambda \cdot p_{\text{inf}}(a)}\right)$

196 3.1 NUMERICAL SIMULATION



211 Figure 2: OBRS calibration results across three views: (a) per-token probability-ratio clipping pulls the
 212 model distribution toward the target, (b) acceptance remains high ($\approx 95\%$) even at large initial KL, and
 213 (c) overall KL is reduced by roughly an order of magnitude.

214 Crucially, this calibration is highly efficient; the acceptance rate remains high even when there is a large
 215 initial KL divergence. The impact on distributional alignment is dramatic: a significant reduction in KL

216 divergence is observed with high acceptance rates. By systematically damping the most extreme probability
 217 ratios, OBRS produces a distribution that is not only provably closer to the on-policy target but also primed
 218 to yield more stable and effective PPO/GRPO policy updates.
 219

220 **3.2 THEORETICAL GUARANTEES**
 221

222 OBRS possesses proven optimality. It has been established that for any desired average acceptance rate
 223 $\bar{\alpha} \in (0, 1]$, there exists a corresponding scaling factor C that achieves it. Crucially, among all possible
 224 rejection rules that satisfy this budget, this scaled acceptance rule is the unique one that **minimizes the**
 225 **Kullback-Leibler (KL) divergence** to the target distribution $p_{\theta_{\text{new}}}$. A formal statement and proof of this
 226 theorem are provided in Appendix §A.2. This guarantee ensures we are using the provably best method
 227 for trading sample efficiency for distributional accuracy.

228 The scaling factor C acts as an explicit control knob for this trade-off. A larger C pushes the post-rejection
 229 distribution closer to the true target $p_{\theta_{\text{new}}}$ at the expense of a lower acceptance rate, while a smaller C boosts
 230 throughput at the cost of higher divergence. In our experiments, we find $C=1$ to be a robust default.

231 This formulation also guarantees that applying this sampling technique is always better than using the original
 232 inference distribution p_{inf} directly. The post-rejection distribution $p_{\text{kept}, C}$ is strictly closer to the target $p_{\theta_{\text{new}}}$ in
 233 KL divergence than the original p_{inf} for any choice of $C > 0$. We provide a summary of this proof tailored to
 234 our notation in Appendix §A. Our algorithm for implementing this procedure is also detailed in Appendix §A.
 235

236
 237 **4 JACKPOT: DESIGN AND METHODOLOGY**
 238

240 In this section, we present details on the design considerations of JACKPOT. We show the token rejection
 241 criteria and reweighting procedures in Section, applying our rejection sampling to the PPO setup in Sections,
 242 and efficiency analysis in Section.
 243

244 **4.1 REJECTION AND REWEIGHTING**
 245

246 To bridge the inference probability distribution p_{inf} and the target distribution p_{target} , we use the following
 247 critieria similar to Leviathan et al. (2023). For token sampled by p_{inf} , x , we accept token with probability
 248

$$\min\left(1, \frac{p_{\text{target}}(x)}{\lambda p_{\text{inf}}(x)}\right). \quad (3)$$

251 Note that the above equation is $P(x \text{ accepted} \mid x \text{ sampled by } p_{\text{inf}}(x))$. Once the token x is rejected, it will
 252 be masked out and no longer participate in the loss and gradient propagation. After rejection, the distribution
 253 has expression:
 254

$$P_{\text{OBRS}} = \frac{\min(p_{\text{inf}}(x), \frac{p_{\text{target}}(x)}{\lambda})}{\sum_{x'} \min(p_{\text{inf}}(x'), \frac{p_{\text{target}}(x')}{\lambda})}. \quad (4)$$

259 **4.2 INTEGRATION WITH CONVENTIONAL PPO OBJECTIVE**
 260

261 Following Section 4.1 , we have the following PPO objective and applied Truncated Importance Sampling,

$$\mathcal{L}_{\text{standard}}^{\text{PPO}}(\theta) = \mathbb{E}_{x \sim p_{\text{inf}}} \left[f(x) \right] = \mathbb{E}_{x \sim P_{\text{inf}}} \left[\min(r_{\theta}(x) \hat{A}(x), \text{clip}(r_{\theta}(x), 1-\epsilon, 1+\epsilon) \hat{A}(x)) \right] \quad (5)$$

$$\mathcal{L}_{\text{TIS}}^{\text{PPO}}(\theta) = \mathbb{E}_{x \sim P_{\text{inf}}} \left[\min\left(\frac{p_{\text{ref}}(x)}{p_{\text{inf}}(x)}, C\right) f(x) \right] \quad (6)$$

266 On top of TIS, we can further corrects the p_{inf} of interest by using our rejection sampling critieria and
 267 reweighting by,
 268

$$\min\left(\frac{p_{\text{ref}}(x)}{p_{\text{inf}}(x)}, C\right) \rightarrow \min\left(\frac{p_{\text{ref}}(x)}{\frac{\min(p_{\text{ref}}(x')/\lambda, p_{\text{inf}}(x'))}{Z}}, C\right) = \min\left(Z \cdot \max\left(\lambda, \frac{p_{\text{ref}}(x)}{p_{\text{inf}}(x)}\right), C\right) \quad (7)$$

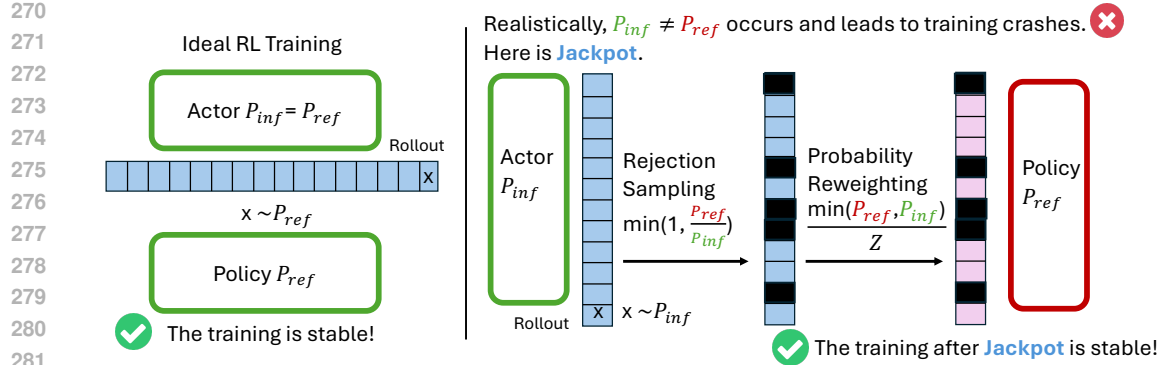


Figure 3: Illustration of JACKPOT Pipeline focusing on Optimal Budgeted Rejection Sampling (OBRS) and Reweighting Procedures

where Z is $\sum_{x'} \min(p_{\text{inf}}(x'), \frac{p_{\text{ref}}(x')}{\lambda})$. Therefore, instead of (6), we use the following PPO objective formulation,

$$\mathcal{L}_{\text{ours}}^{\text{PPO}}(\theta) = \mathbb{E}_{x \sim P_{\text{inf}}} \left[\min(Z \cdot \max(\lambda, \frac{p_{\text{ref}}(x)}{p_{\text{inf}}(x)}), C) \cdot f(x) \right] \quad (8)$$

4.3 WHICH POLICY TO APPROXIMATE?

Conventionally, we assume $p_{\text{inf}} = p_{\text{ref}}$, but empirically, we discover that for settings where RL training suffers from severe staleness, e.g. using large batch size or using asynchronous rollout/update cycles, approximating $p_{\text{inf}} \rightarrow p_{\text{new}}$ the latest updated policy edges out in performance. The rationale is that the reference policy is too stale and too distant to the latest updated policy to offer reliable trust region. In that case, we adjust the conventional PPO objective in (2) to the following from importance sampling,

$$\mathbb{E}_{x \sim P_{\text{ref}}} [f(x)] = \mathbb{E}_{x \sim P_{\text{new}}} \left[\frac{p_{\text{ref}}}{p_{\text{new}}} f(x) \right] \quad (9)$$

Then, we can approximate p_{new} using p_{inf} through our rejection sampling and reweighting. For the high staleness settings, we use the following approximating formulation,

$$\mathbb{E}_{x \sim P_{\text{new}}} \left[\frac{p_{\text{ref}}}{p_{\text{new}}} f(x) \right] \leftarrow \mathbb{E}_{x \sim P_{\text{inf}}} \left[\min \left(\frac{p_{\text{new}}}{p_{\text{inf}}^*}, C_1 \right) \cdot \min \left(\frac{p_{\text{ref}}}{p_{\text{new}}}, C_2 \right) \cdot f(x) \right] \quad (10)$$

where p_{inf}^* is the corrected distribution through rejection sampling and reweighting.

We then have the JACKPOT objective,

$$\mathcal{L}_{\text{ours}}^{\text{PPO}}(\theta) = \left[\min(Z \cdot \max(\lambda, \frac{p_{\text{new}}(x)}{p_{\text{inf}}(x)}), C_1) \cdot \min(\frac{p_{\text{ref}}}{p_{\text{new}}}, C_2) \cdot f(x) \right] \quad (11)$$

Throughout our experiments, we use $\lambda = 1$. We offer the user to either use (8) to align to p_{ref} or p_{new} depending on their target policy desired under their use cases.

4.4 STABILIZATION AND FEASIBILITY CHALLENGES

Implementing JACKPOT directly faces a huge challenge of computational feasibility. Note that the weight's normalization constant, Z , requires a sum over the entire vocabulary ($|\mathcal{V}| > 100,000$), creating a crippling memory bottleneck from storing full logit vectors ($\text{batch_size} \times \text{seq_len} \times \text{vocab_size}$). This severely restricts batch sizes, directly undermining the efficiency OBRS is intended to provide. Therefore, transforming this principled approach into a production-ready algorithm requires non-trivial engineering: we must introduce mechanisms to both bound the importance weights for stability and develop a computationally efficient, low-bias estimator for the normalization constant. To overcome the computational bottleneck of calculating Z , we employ a top-k approximation, which we then de-bias empirically.

4.4.1 TOP-K APPROXIMATION

The probability mass of language models is typically concentrated in a small subset of the vocabulary. We leverage this property by approximating the sum over \mathcal{V} with a sum over a much smaller set, \mathcal{V}_k , which

324 contains the most likely tokens from both the inference and current policies. Specifically, let $\text{top-}k(p)$ be the
 325 set of k tokens with the highest probability under distribution p . We define our approximation set as the union:
 326

$$\mathcal{V}_k = \text{top-}k(p_{\text{inf}}) \cup \text{top-}k(p_{\theta_{\text{new}}})$$

327 The union is crucial because a token might be highly probable under one distribution but not the other, and the
 328 min function makes these overlapping regions important. The approximate normalization constant, Z_{approx} ,
 329 is then: $Z_{\text{approx}} = \sum_{a' \in \mathcal{V}_k} \min\left(p_{\text{inf}}(a'), \frac{p_{\text{target}}(a')}{\lambda}\right)$
 330

331 4.4.2 BIAS CORRECTION

333 While efficient, this top- k approximation introduces a systematic bias. Since the terms in the sum are
 334 non-negative, omitting tokens from the full vocabulary \mathcal{V} can only decrease the total sum. Therefore, our
 335 approximation is a consistent underestimation of the true value:

$$\mathbb{E}[Z_{\text{approx}}] \leq Z$$

337 For $k=20$, . This bias could systematically alter the scale of the gradients during training. Fortunately, there
 338 is an elegant way to correct this. A key property of the framework is that the true normalization constant
 339 Z is exactly equal to the expected acceptance rate, $\bar{\alpha}$:

$$340 \bar{\alpha} = \sum_{a \in \mathcal{V}} p_{\text{inf}}(a) \cdot \min\left(1, \frac{p_{\text{target}}(a)}{\lambda \cdot p_{\text{inf}}(a)}\right) = \sum_{a \in \mathcal{V}} \min\left(p_{\text{inf}}(a), \frac{p_{\text{target}}(a)}{\lambda}\right) = Z.$$

342 During the data collection phase (Algorithm 1, Phase 1), we can compute an unbiased empirical estimate
 343 of $\bar{\alpha}$ from the observed samples:

$$344 \hat{\bar{\alpha}} = \frac{\text{Number of accepted samples}}{\text{Total number of proposed samples}}$$

346 This gives us two estimators for Z : the low-variance but biased Z_{approx} , and the unbiased but higher-variance
 347 $\hat{\bar{\alpha}}$. We can combine them to create a de-biased, low-variance estimator. We compute a batch-wide calibration
 348 factor, κ , by dividing the empirical acceptance rate by the batch-averaged Z_{approx} :

$$349 \kappa = \frac{\hat{\bar{\alpha}}}{\frac{1}{B} \sum_{i=1}^B Z_{\text{approx}}^{(i)}}$$

352 where B is the number of samples in the batch. We then apply this scalar correction to each per-token Z_{approx}
 353 value used in the loss calculation. This procedure scales our efficient top- k estimate to match the true expected
 354 value observed in practice, effectively removing the bias while retaining the computational benefits and
 355 lower variance of the top- k approach.

356 4.5 IMPLEMENTATION OVERHEAD ANALYSIS

358 JACKPOT is lightweight. First, JACKPOT requires no additional trajectories sampled, as all the experiments we
 359 conducted in the extensive empirical studies section are using the same rollout width as the on-policy baseline.
 360 **A critical distinction to Leviathan et al. (2023) is that JACKPOT doesn't reject all tokens from the first**
 361 **place in the trajectory where a token first rejects and resample from where. Instead, JACKPOT only**
 362 **mask out tokens using our rejection critieria, and no additional trajectories sampling needed.** Second,
 363 no additional `log_prob` computation needed, since both p_{ref} and p_{new} will be computed by the standard
 364 objective (5), and JACKPOT only needs to reuse these probability distributions already computed. Third, no
 365 modification required on vLLM. Since JACKPOT doesn't required special operator or numeric precisions, we
 366 directly based our implementation on standard vLLM for rollout, without relying on custom kernels in vLLM.

367 JACKPOT indeed add minor additional overhead to standard PPO objective computation. The added
 368 computation comes from forcing vLLM to return `top-K` logprobs. Fortunately, since we only use $k=20$
 369 for our runs, the added extra compute only added less than 3% to the total compute. In contrast, JACKPOT
 370 helps models be trained using $64\times$ or higher batch sizes by drastically alleviating the lack of convergence
 371 from the staleness of the actor model. Thus, comparing with the small batch and on-policy performance,
 372 we achieve more than 4 times speedup.

373 5 EMPIRICAL VALIDATION

376 In this section, we comprehensively test our method on two different and challenging misalignment settings.
 377 First, we evaluate our method on an extremely large inference batch size, while keeping the training
 378 mini-batch size the same. At the end of each training-inference cycle, the staleness of the model weights

378 **Algorithm 1** The Jackpot Algorithm

379

380 **Require:** Policies: current p_{new} , reference p_{ref} , inference p_{inf} .

381 **Require:** Hyperparameters: OBRS threshold λ , PPO clip ϵ , Jackpot clips c_1, c_2 , top- k count.

382 1: **Convention:** $\text{SG}(\cdot)$ denotes the stop-gradient operation.

383 2: **Implementation note:** Jackpot only reweights quantities from the *standard* rollout and PPO/GRPO

384 forward passes; it does *not* perform extra model forward passes or trajectory recomputation.

385 3: **Phase 1: Efficient Rollout (Standard Generation)**

386 4: Initialize experience buffer $\mathcal{D} \leftarrow \emptyset$.

387 5: **for** each trajectory sampling step t **do**

388 6: Single forward pass of $p_{\text{inf}}(\cdot | s_t)$, sample $a_t \sim p_{\text{inf}}(\cdot | s_t)$.

389 7: From the same forward, compute and store top- k log-probabilities of p_{inf} : $\text{TopK}_{\text{inf}}(s_t)$.

390 8: Store $(s_t, a_t, p_{\text{inf}}(a_t | s_t), \text{TopK}_{\text{inf}}(s_t))$ (plus rewards, values, etc.) in buffer \mathcal{D} .

391 9: **end for**

392 10: Compute advantages \hat{A}_t using collected trajectories.

393 11: **Phase 2: PPO Update with Jackpot Reweighting**

394 12: **for** each mini-batch sampled from \mathcal{D} **do**

395 13: // 1. Standard PPO Computation (reused by Jackpot)

396 14: Forward pass p_{new} and p_{ref} on the mini-batch to get logits, $p_{\text{new}}(a_t | s_t)$, $p_{\text{ref}}(a_t | s_t)$, and $\text{TopK}_{\text{new}}(s_t)$.

397 15: Compute policy ratio: $r_t(\theta) = \frac{p_{\text{new}}(a_t | s_t)}{p_{\text{ref}}(a_t | s_t)}$.

398 16: Compute vanilla PPO objective: $\mathcal{L}_{\text{PPO}} = \min(r_t(\theta) \hat{A}_t, \text{clip}(r_t(\theta), 1 - \epsilon, 1 + \epsilon) \hat{A}_t)$.

399 17: // 2. Efficient Z-Approximation and Bias Correction (no extra forward passes)

400 18: Construct approximation set $\mathcal{V}_k = \text{TopK}_{\text{inf}}(s_t) \cup \text{TopK}_{\text{new}}(s_t)$.

401 19: Compute

402
$$Z_{\text{approx}} = \sum_{x \in \mathcal{V}_k} \min\left(p_{\text{inf}}(x | s_t), \frac{p_{\text{new}}(x | s_t)}{\lambda}\right).$$

403

404 20: Estimate correction factor κ using the OBRS-based bias-correction procedure described in Sec. 4.4.2

405 (e.g., from batch-level OBRS statistics).

406 21: Set corrected normalizer $Z_t \leftarrow \kappa \cdot Z_{\text{approx}}$.

407 22: // 3. Jackpot Weight Calculation

408 23: OBRS weight: $w_{\text{OBRS}} = Z_t \cdot \max\left(\lambda, \frac{p_{\text{new}}(a_t | s_t)}{p_{\text{inf}}(a_t | s_t)}\right)$.

409 24: $\rho_{\text{jackpot}} = \min(w_{\text{OBRS}}, c_1) \cdot \min\left(\frac{p_{\text{ref}}(a_t | s_t)}{p_{\text{new}}(a_t | s_t)}, c_2\right)$.

410 25: // 4. Apply Weight to Loss

411 26: $\mathcal{L}_{\text{final}} = \text{SG}(\rho_{\text{jackpot}}) \cdot \mathcal{L}_{\text{PPO}}$.

412 27: Update policy parameters new using gradient of $-\mathcal{L}_{\text{final}}$.

413 28: **end for**

414

415

416 in the inference server will be significantly amplified. Secondly, we evaluate our method using two separate

417 models for training and rollout, an extreme setting where the output distribution gap is more severe than

418 usual staleness in off-policy RL settings. We show that our technique enables the training model to better

419 benefit from tokens from a completely distinct model. [Because of the limit in space, we list detailed ablation](#)

420 [studies on threshold selection and top-K analysis in the Appendix C.](#)

421

422 5.1 INFERENCE WITH LARGE BATCH SIZE AND TRAINING WITH MUCH SMALLER BATCH SIZE

423

424 RL training using a much larger batch size for generation and a smaller batch size for training is common

425 in practice. It is usually due to either system limitation, where the generation is highly parallelizable and

426 relatively memory-light compared to training (saving optimizer states, etc.), or it is for better stability as

427 advocated by Schulman et al. (2017). However, the delay in updates results in staleness, which we magnify

428 for evaluating our method.

429 We use the best results under 30k examples for Qwen3-4B-Base as our metrics, and the best under 50k

430 for Qwen3-8B-Base. ¹. The results of our run are summarized in table 1. On-policy RL generally converges

431

¹Qwen3-4B-Base on-policy run crashes at 30k examples.

Table 1: Evaluation scores across benchmarks. TIS + Adjustment is explained in Section B.1.

Models / Methods	GSM8K	MATH-500	AMC22 & 23	AMC12 2024	AIME24		AIME25	
	Mean@4	Mean@4	Mean@4	Mean@4	Mean@16	Pass@16	Mean@16	Pass@16
Qwen3-4B-Base on DeepScaleR-Preview Dataset (rollout batch size = 2048; train batch size = 32; 64 \times)								
On Policy	92.19	81.55	58.43	51.11	23.12	33.13	22.91	30.95
Off Policy	88.04	71.15	39.15	29.44	13.96	23.03	11.04	18.61
TIS	89.67	72.00	42.77	31.67	11.88	17.56	11.25	17.28
TIS + Adjustment	92.76	79.50	57.22	43.33	18.75	26.03	17.71	24.61
Jackpot (Ours)	92.24	80.05	53.92	50.00	20.63	29.48	18.13	23.63
Qwen3-4B-Base on DeepScaleR-Preview Dataset (rollout batch size = 4096; train batch size = 32; 128 \times)								
Off Policy	79.70	60.20	33.00	24.44	8.00	15.73	5.00	11.00
TIS + Adjustment	20.70	19.10	7.80	5.00	1.00	4.00	1.00	2.00
Jackpot (Ours)	92.00	80.00	51.20	47.22	19.16	24.58	18.52	25.08
Qwen3-8B-Base on DeepScaleR-Preview Dataset (rollout batch size = 2048; train batch size = 32; 64 \times)								
On Policy	94.24	93.99	28.95	54.44	28.95	37.89	22.50	28.54
Off Policy	91.05	77.15	50.60	40.00	18.54	28.67	14.16	21.98
TIS + Adjustment	93.85	82.55	60.54	48.33	24.58	35.06	20.00	22.90
Jackpot (Ours)	94.01	83.05	63.55	54.44	26.87	36.23	20.41	26.57

Table 2: AMC22&23 results of two model training using various methods across the training steps. Mean@k/Pass@k.

AMC22 & 23	Rollout Model	Train Model	0	20	30	40	50	60	70
Vanilla GRPO	Q2.5-1.5B-IT	Qwen2.5-3B-Base	18.1/48.2	31.8/59.0	32.2/61.5	33.3/59.0	30.0/49.4	22.4/42.3	5.7/16.9
TIS	Qwen2.5-1.5B-IT	Q2.5-3B-Base	18.1/48.2	28.9/57.8	28.2/54.2	32.5/68.7	26.8/56.6	0/0	0/0
Jackpot (ours)	Q2.5-1.5B-IT	Qwen2.5-3B-Base	18.1/48.2	29.4/59.0	31.2/57.8	33.9/60.2	31.9/62.7	28.8/54.2	13.4/31.3
AMC22 & 23	Rollout Model	Train Model	0	20	30	40	50	60	70
Vanilla GRPO	Q2.5-MATH-1.5B-IT	Qwen2.5-3B-Base	18.1/48.2	23.3/60.2	22.6/57.8	24.7/53.0	17.0/43.4	3.9/14.5	0
TIS	Q2.5-MATH-1.5B-IT	Qwen2.5-3B-Base	18.1/48.2	25.8/59	25.0/59.0	21.7/55.4	0	0	0
Jackpot (ours)	Q2.5-MATH-1.5B-IT	Qwen2.5-3B-Base	18.1/48.2	27.3/57.8	29.4/63.9	26.7/59.0	28.6/60.2	22.4/54.2	2.9/16.9

much faster than off-policy runs. We observed that for less aggressive off-policy settings, our method's margin is quite small. However, for extreme settings, such as 4096-32 for Qwen3-4B-Base and 2048-32 for Qwen3-8B-Base. We observed consistently that TIS-adjusted crashes occurred way earlier than our settings, often resulting in inferior results. For example, Qwen3-4B-Base TIS-adjusted fails to converge from the beginning. Also, as shown in Figure fig. 4 (a), TIS-adjusted also crashes way earlier than ours under the 2048-32 setting. Across all settings we tested, our method greatly improves the speed of convergence of the off-policy RL, while also resulting in performance numbers comparable to the on-policy runs.

Besides, as a much less aggressive setting, KV FP8 quantization can result in a performance crash as shown in Figure 4(b). Here, we apply only our rejection sampling algorithm, without clipping/truncation or any similar tricks. We show our performance recovers from crashes.

5.2 EXTREME OFFPOLICY SETTINGS

In this section, we demonstrate our method's effectiveness on the extreme setting where the model under inference and training are fundamentally two separate models. Specifically, we hypothesize that our sampling algorithm can always filter out useful tokens for the model training, even given a completely exotic output response. We use Qwen2.5-3B-Base as the trainer model, and we adopt different inference models from Qwen2.5-1.5B-Instruct to Qwen2.5-Math-1.5B-Instruct, trained on MATH-8K Hendrycks et al. (2021) dataset. We find out that our method can still improve itself under such extreme settings.

Shown in Figure 4 (c), we see that our run green curve shows clear improvement over our baseline GRPO and TIS settings. It even increases by 12% on MATH-500 under such an extreme misaligned setting. More results are summarized in Table 2, showing that the improvement also exists on AMC problems. We believe our method offers a new possibility to unlock much more scalability in RL efficiency and performance.

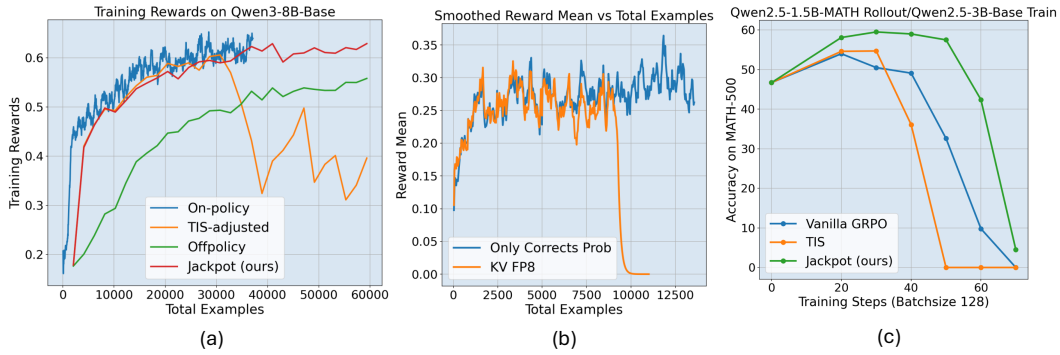


Figure 4: Overview of our empirical experiment results. (a) shows our proposed method’s strength in correcting stale inference model distribution, and approaches the on-policy trend while maintaining training stability; (b) shows our proposed method to align output distribution can correct RL training instability even if applied alone; (c) The strength in our model’s ability to align two different distributions allows us to put it in the most extremely misalignment setting where the rollout and the training model are separate of different architecture, our method shows early glimpse of hope and beats the baseline.

6 CONCLUSION

We propose Jackpot, which leverages Optimal Budget Rejection Sampling to directly reduce the gap between actor and policy distribution. Empirically, our method achieves stable improvements in large-batch and asynchronous training and also demonstrates stability under extreme misalignment settings.

510
511
512
513
514
515
516
517
518
519
520
521
522
523
524
525
526
527
528
529
530
531
532
533
534
535
536
537
538
539

540 7 ETHICS STATEMENT
541

542 Our study is centered on the development of reinforcement learning techniques for large language models.
 543 The research does not involve the use of human subjects, personal data, or other sensitive information. All
 544 datasets employed are openly accessible and commonly utilized within the research community. We recognize
 545 that advancements in LLMs may lead to societal risks, such as the potential misuse for generating harmful
 546 or deceptive outputs. To address such concerns, this work is conducted strictly within controlled academic
 547 environments, with the primary objective of enhancing the robustness and efficiency of training methodologies.
 548

549 8 REPRODUCIBILITY STATEMENT
550

551 We have provided a comprehensive account of implementation details, hyperparameters, and experimental
 552 configurations in both the main text and the appendix. This documentation is intended to ensure that other
 553 researchers are able to independently reproduce our findings without ambiguity.
 554

555 REFERENCES
556

557 Arash Ahmadian, Chris Cremer, Matthias Gallé, Marzieh Fadaee, Julia Kreutzer, Olivier Pietquin, Ahmet
 558 Üstün, and Sara Hooker. Back to basics: Revisiting reinforce style optimization for learning from human
 559 feedback in llms. *arXiv preprint arXiv:2402.14740*, 2024.

560 Zhangir Azerbayev, Hailey Schoelkopf, Keiran Paster, Marco Dos Santos, Stephen McAleer, Albert Q Jiang,
 561 Jia Deng, Stella Biderman, and Sean Welleck. Llemma: An open language model for mathematics. *arXiv
 562 preprint arXiv:2310.10631*, 2023.

563 Ernesto Carrella, Joseph Powers, Steven Saul, Richard M Bailey, Nicolas Payette, Katanya A Vert-pre, Aarthi
 564 Ananthanarayanan, Michael Drexler, Chris Dorsett, and Jens Koed Madsen. Rejection sampling and
 565 agent-based models for data limited fisheries. *Frontiers in Marine Science*, 11:1243954, 2024.

566 Lasse Espeholt, Hubert Soyer, Remi Munos, Karen Simonyan, Volodymir Mnih, Tom Ward, Yotam
 567 Doron, Vlad Firoiu, Tim Harley, Iain Dunning, Shane Legg, and Koray Kavukcuoglu. Impala:
 568 Scalable distributed deep-rl with importance weighted actor-learner architectures, 2018. URL
 569 <https://arxiv.org/abs/1802.01561>.

570 Wei Fu, Jiaxuan Gao, Xujie Shen, Chen Zhu, Zhiyu Mei, Chuyi He, Shusheng Xu, Guo Wei, Jun Mei, Jiashu
 571 Wang, et al. Areal: A large-scale asynchronous reinforcement learning system for language reasoning.
 572 *arXiv preprint arXiv:2505.24298*, 2025.

573 Wally R Gilks, Nicky G Best, and Keith KC Tan. Adaptive rejection metropolis sampling within gibbs
 574 sampling. *Journal of the Royal Statistical Society Series C: Applied Statistics*, 44(4):455–472, 1995.

575 Daya Guo, Dejian Yang, Haowei Zhang, Junxiao Song, Ruoyu Zhang, Runxin Xu, Qihao Zhu, Shirong
 576 Ma, Peiyi Wang, Xiao Bi, et al. Deepseek-rl: Incentivizing reasoning capability in llms via reinforcement
 577 learning. *arXiv preprint arXiv:2501.12948*, 2025.

578 Horace He and Thinking Machines Lab. Defeating nondeterminism in llm inference. *Thinking Machines
 579 Lab: Connectionism*, 2025. doi: 10.64434/tml.20250910. [https://thinkingmachines.ai/blog/defeating-
 nondeterminism-in-llm-inference/](https://thinkingmachines.ai/blog/defeating-

 580 nondeterminism-in-llm-inference/).

581 Dan Hendrycks, Collin Burns, Saurav Kadavath, Akul Arora, Steven Basart, Eric Tang, Dawn Song,
 582 and Jacob Steinhardt. Measuring mathematical problem solving with the math dataset, 2021. URL
 583 <https://arxiv.org/abs/2103.03874>.

584 Jian Hu, Xibin Wu, Zilin Zhu, Xianyu, Weixun Wang, Dehao Zhang, and Yu Cao. Openrlhf: An easy-to-use,
 585 scalable and high-performance rlhf framework. *arXiv preprint arXiv:2405.11143*, 2024.

586 Carlos E Jimenez, John Yang, Alexander Wettig, Shunyu Yao, Kexin Pei, Ofir Press, and Karthik Narasimhan.
 587 Swe-bench: Can language models resolve real-world github issues? *arXiv preprint arXiv:2310.06770*, 2023.

588 Yann Leviathan, Matan Kalman, and Yossi Matias. Fast inference from transformers via speculative decoding.
 589 In *International Conference on Machine Learning*, pp. 19274–19286. PMLR, 2023.

594 Ziniu Li, Tian Xu, Yushun Zhang, Zhihang Lin, Yang Yu, Ruoyu Sun, and Zhi-Quan Luo. Remax: A simple,
 595 effective, and efficient reinforcement learning method for aligning large language models. *arXiv preprint*
 596 *arXiv:2310.10505*, 2023.

597

598 Liyuan Liu, Feng Yao, Dinghuai Zhang, Chengyu Dong, Jingbo Shang, and Jianfeng Gao. Flashrl: 8bit
 599 rollouts, full power rl, August 2025. URL <https://fengyao.notion.site/flash-rl>.

600

601 Xiao Liu, Hao Yu, Hanchen Zhang, Yifan Xu, Xuanyu Lei, Hanyu Lai, Yu Gu, Hangliang Ding, Kaiwen Men,
 602 Kejuan Yang, Shudan Zhang, Xiang Deng, Aohan Zeng, Zhengxiao Du, Chenhui Zhang, Sheng Shen,
 603 Tianjun Zhang, Yu Su, Huan Sun, Minlie Huang, Yuxiao Dong, and Jie Tang. Agentbench: Evaluating
 604 llms as agents. *arXiv preprint arXiv: 2308.03688*, 2023.

605

606 Michael Luo, Sijun Tan, Justin Wong, Xiaoxiang Shi, William Y. Tang, Manan Roongta, Colin Cai, Jeffrey
 607 Luo, Li Erran Li, Raluca Ada Popa, and Ion Stoica. Deepscaler: Surpassing o1-preview with a 1.5b model
 608 by scaling rl, 2025. Notion Blog.

609

610 Luca Martino and Joaquín Míguez. A generalization of the adaptive rejection sampling algorithm. *Statistics
 and Computing*, 21(4):633–647, 2011.

611

612 Yu Meng, Mengzhou Xia, and Danqi Chen. Simpo: Simple preference optimization with a reference-free
 613 reward. *Advances in Neural Information Processing Systems*, 37:124198–124235, 2024.

614

615 Christian A Naesseth, Francisco JR Ruiz, Scott W Linderman, and David M Blei. Rejection sampling
 616 variational inference. *stat*, 1050:18, 2016.

617

618 Anne Ouyang, Simon Guo, Simran Arora, Alex L Zhang, William Hu, Christopher Ré, and Azalia Mirhoseini.
 619 Kernelbench: Can llms write efficient gpu kernels? *arXiv preprint arXiv:2502.10517*, 2025.

620

621 Rafael Rafailov, Archit Sharma, Eric Mitchell, Christopher D Manning, Stefano Ermon, and Chelsea Finn.
 622 Direct preference optimization: Your language model is secretly a reward model. *Advances in neural
 623 information processing systems*, 36:53728–53741, 2023.

624

625 John Schulman, Filip Wolski, Prafulla Dhariwal, Alec Radford, and Oleg Klimov. Proximal policy
 626 optimization algorithms, 2017. URL <https://arxiv.org/abs/1707.06347>.

627

628 Zhihong Shao, Peiyi Wang, Qihao Zhu, Runxin Xu, Junxiao Song, Xiao Bi, Haowei Zhang, Mingchuan
 629 Zhang, YK Li, Yang Wu, et al. Deepseekmath: Pushing the limits of mathematical reasoning in open
 language models. *arXiv preprint arXiv:2402.03300*, 2024.

630

631 Guangming Sheng, Chi Zhang, Zilingfeng Ye, Xibin Wu, Wang Zhang, Ru Zhang, Yanghua Peng, Haibin
 632 Lin, and Chuan Wu. Hybridflow: A flexible and efficient rlhf framework. In *Proceedings of the Twentieth
 633 European Conference on Computer Systems*, pp. 1279–1297, 2025.

634

635 Alexandre Verine, Muni Sreenivas Pydi, Benjamin Negrevergne, and Yann Chevaleyre. Optimal budgeted
 636 rejection sampling for generative models. In *International Conference on Artificial Intelligence and
 637 Statistics*, pp. 3367–3375. PMLR, 2024.

638

639 Leandro von Werra, Younes Belkada, Lewis Tunstall, Edward Beeching, Tristan Thrush, Nathan Lambert,
 640 Shengyi Huang, Kashif Rasul, and Quentin Gallouédec. Trl: Transformer reinforcement learning.
 641 <https://github.com/huggingface/trl>, 2020.

642

643 Bo Wu, Sid Wang, Yunhao Tang, Jia Ding, Eryk Helenowski, Liang Tan, Tengyu Xu, Tushar Gowda,
 644 Zhengxing Chen, Chen Zhu, Xiaocheng Tang, Yundi Qian, Beibei Zhu, and Rui Hou. Llamarl: A
 645 distributed asynchronous reinforcement learning framework for efficient large-scale llm training, 2025a.
 646 URL <https://arxiv.org/abs/2505.24034>.

647

648 Bo Wu, Sid Wang, Yunhao Tang, Jia Ding, Eryk Helenowski, Liang Tan, Tengyu Xu, Tushar Gowda,
 649 Zhengxing Chen, Chen Zhu, et al. Llamarl: A distributed asynchronous reinforcement learning framework
 650 for efficient large-scale llm trainin. *arXiv preprint arXiv:2505.24034*, 2025b.

648 An Yang, Anfeng Li, Baosong Yang, Beichen Zhang, Binyuan Hui, Bo Zheng, Bowen Yu, Chang Gao,
 649 Chengen Huang, Chenxu Lv, Chujie Zheng, Dayiheng Liu, Fan Zhou, Fei Huang, Feng Hu, Hao Ge,
 650 Haoran Wei, Huan Lin, Jialong Tang, Jian Yang, Jianhong Tu, Jianwei Zhang, Jianxin Yang, Jiaxi Yang,
 651 Jing Zhou, Jingren Zhou, Junyang Lin, Kai Dang, Keqin Bao, Kexin Yang, Le Yu, Lianghao Deng,
 652 Mei Li, Mingfeng Xue, Mingze Li, Pei Zhang, Peng Wang, Qin Zhu, Rui Men, Ruize Gao, Shixuan
 653 Liu, Shuang Luo, Tianhao Li, Tianyi Tang, Wenbiao Yin, Xingzhang Ren, Xinyu Wang, Xinyu Zhang,
 654 Xuancheng Ren, Yang Fan, Yang Su, Yichang Zhang, Yingqi Zhang, Yu Wan, Yuqiong Liu, Zekun
 655 Wang, Zeyu Cui, Zhenru Zhang, Zhipeng Zhou, and Zihan Qiu. Qwen3 technical report, 2025. URL
 656 <https://arxiv.org/abs/2505.09388>.

657 Chujie Zheng, Shixuan Liu, Mingze Li, Xiong-Hui Chen, Bowen Yu, Chang Gao, Kai Dang, Yuqiong Liu,
 658 Rui Men, An Yang, et al. Group sequence policy optimization. *arXiv preprint arXiv:2507.18071*, 2025a.

659 Haizhong Zheng, Yang Zhou, Brian R Bartoldson, Bhavya Kailkhura, Fan Lai, Jiawei Zhao, and Beidi Chen.
 660 Act only when it pays: Efficient reinforcement learning for llm reasoning via selective rollouts. *arXiv
 661 preprint arXiv:2506.02177*, 2025b.

663 A ANALYSIS OF OBR^S

664 This appendix provides the theoretical foundation for OBR^S. We first formally define the post-rejection
 665 distribution that results from our method. We then prove two key results:

- 666 1. **Optimality:** For any desired sample efficiency (i.e., acceptance rate), OBR^S is the unique optimal
 667 rejection mechanism that produces a post-rejection distribution closest to the target $p_{\theta_{\text{new}}}$ in terms
 668 of KL divergence (Theorem 1).
- 669 2. **Monotonic Improvement:** The post-rejection distribution monotonically approaches the target
 670 distribution as the scaling factor C increases. This guarantees that for any $C > 0$, OBR^S reduces
 671 the KL divergence compared to using the proposal p_{inf} directly. (Proposition 1).

672 For notational clarity, we consider the distributions over tokens for a single, fixed prompt and omit the explicit
 673 conditioning. Let $p_t \equiv p_{\theta_{\text{new}}}$ denote the target distribution and $p_p \equiv p_{\text{inf}}$ denote the proposal distribution.

674 **Algorithm 2** Implementation of Optimal Budgeted Rejection Sampling

675 **Require:** Proposal distribution p_{inf} , Target distribution $p_{\theta_{\text{new}}}$
 676 **Require:** Scaling factor $C > 0$, Number of samples to accept N
 677 **Ensure:** Set of accepted samples S_{kept}

- 678 1: Initialize $S_{\text{kept}} \leftarrow \emptyset$
- 679 2: **while** $|S_{\text{kept}}| < N$ **do**
- 680 3: Sample a token $a \sim p_{\text{inf}}(\cdot)$
- 681 4: Calculate acceptance probability $\alpha \leftarrow \min\left(1, \frac{p_{\theta_{\text{new}}}(a)}{C \cdot p_{\text{inf}}(a)}\right)$
- 682 5: **if** $U(0,1) < \alpha$ **then**
- 683 6: Add a to S_{kept}
- 684 7: **end if**
- 685 8: **end while**
- 686 9:
- 687 10: **return** S_{kept}

693 A.1 THE POST-REJECTION DISTRIBUTION

694 Recall from Definition 1 that OBR^S accepts a token $a \sim p_p(a)$ with probability $\alpha_C(a) = \min\left(1, \frac{p_t(a)}{C \cdot p_p(a)}\right)$.
 695 The unnormalized probability of sampling and keeping a token a is $p_p(a) \cdot \alpha_C(a)$, which simplifies to
 696 $\min\{p_p(a), p_t(a)/C\}$.

697 The overall probability of accepting any token, which we denote as the acceptance rate Z_C , is the sum over
 698 all possible tokens:

699
$$700 Z_C = \sum_{a \in \mathcal{A}} \min\left\{p_p(a), \frac{p_t(a)}{C}\right\}.$$

702 The distribution of the tokens that are kept, which we call the post-rejection distribution $p_{\text{kept},C}$, is therefore:
 703

$$704 p_{\text{kept},C}(a) = \frac{\min\{p_p(a), p_t(a)/C\}}{Z_C}.$$

705 Special cases clarify the role of C : as $C \rightarrow 0$, $Z_C \rightarrow 1$ and $p_{\text{kept},C} \rightarrow p_p$ (all tokens are kept). As $C \rightarrow \infty$,
 706 $Z_C \rightarrow 0$ and $p_{\text{kept},C} \rightarrow p_t$ (perfect alignment with vanishing throughput). Standard rejection sampling is
 707 the special case where $C \geq \max_a(p_t(a)/p_p(a))$.
 708

709 A.2 OPTIMALITY FOR A FIXED ACCEPTANCE BUDGET

711 We first establish that OBRS is not merely a heuristic but is the provably optimal strategy for minimizing
 712 distributional error given a fixed efficiency budget.

713 **Theorem 1** (Budgeted Optimal Acceptance). *Fix a target acceptance rate (budget) $z \in (0, 1]$.
 714 Among all possible token-wise acceptance rules $\alpha : \mathcal{A} \rightarrow [0, 1]$ that satisfy the budget constraint
 715 $\mathbb{E}_{a \sim p_p}[\alpha(a)] = \sum_a p_p(a)\alpha(a) = z$, the rule that generates a post-rejection distribution $p_{\text{kept}}(a) \propto p_p(a)\alpha(a)$
 716 minimizing the Kullback-Leibler (KL) divergence $\text{KL}(p_t || p_{\text{kept}})$ is uniquely given by the OBRS rule:*

$$717 \alpha^*(a) = \min\left(1, \frac{p_t(a)}{\lambda \cdot p_p(a)}\right)$$

719 for some constant $\lambda > 0$ (equivalent to C) whose value is determined by the budget z .
 720

721 *Proof.* The post-rejection distribution is $p_{\text{kept}}(a) = p_p(a)\alpha(a)/z$. The KL divergence is:
 722

$$723 \text{KL}(p_t || p_{\text{kept}}) = \sum_a p_t(a) \log \frac{p_t(a)}{p_{\text{kept}}(a)} \\ 724 = \sum_a p_t(a) \log \frac{p_t(a)}{p_p(a)\alpha(a)/z} \\ 725 = \underbrace{\sum_a p_t(a) \log \frac{p_t(a)}{p_p(a)}}_{\text{constant w.r.t. } \alpha} + \log z - \sum_a p_t(a) \log \alpha(a). \\ 726 \\ 727 \\ 728 \\ 729 \\ 730$$

731 Minimizing $\text{KL}(p_t || p_{\text{kept}})$ is therefore equivalent to maximizing $\sum_a p_t(a) \log \alpha(a)$ subject to the constraints:
 732

- 733 1. $\sum_a p_p(a)\alpha(a) = z$ (budget constraint)
- 734 2. $0 \leq \alpha(a) \leq 1$ for all $a \in \mathcal{A}$ (valid probability constraint)

736 This is a convex optimization problem. The Lagrangian is:
 737

$$738 \mathcal{L} = -\sum_a p_t(a) \log \alpha(a) + \lambda \left(\sum_a p_p(a)\alpha(a) - z \right) + \sum_a \mu_a(\alpha(a) - 1) - \sum_a \nu_a \alpha(a)$$

739 where λ, μ_a, ν_a are the KKT multipliers. From the stationarity condition $\frac{\partial \mathcal{L}}{\partial \alpha(a)} = 0$, we get $-\frac{p_t(a)}{\alpha(a)} + \lambda p_p(a) + \mu_a - \nu_a = 0$. The complementary slackness conditions imply that if $0 < \alpha(a) < 1$, then $\mu_a = \nu_a = 0$, which gives $\alpha(a) = \frac{p_t(a)}{\lambda p_p(a)}$. If $\alpha(a) = 1$, then $\nu_a = 0$, which requires $\lambda p_p(a) \geq p_t(a)$. If $\alpha(a) = 0$, this form is not well-defined, but the logic holds. Combining these cases, the optimal rule is to cap the acceptance ratio at 1:
 740

$$741 \alpha^*(a) = \min\left(1, \frac{p_t(a)}{\lambda p_p(a)}\right).$$

742 The Lagrange multiplier λ is chosen to meet the budget constraint $\sum_a p_p(a)\alpha^*(a) = z$. Uniqueness follows
 743 from the strict concavity of the log objective function. \square
 744

745 A.3 GUARANTEED KL DIVERGENCE REDUCTION

751 Next, we show that our method provides a guaranteed improvement over the proposal distribution p_p and
 752 that this improvement is monotonic in the control parameter C .
 753

754 **Proposition 1** (Monotonic KL Contraction). *The function $G(C) = \text{KL}(p_t || p_{\text{kept},C})$ is non-increasing for
 755 $C \in (0, \infty)$. It is strictly decreasing wherever the set of tokens $\{a | p_t(a) < C \cdot p_p(a)\}$ has non-zero probability
 756 mass under p_t .*

756 *Proof.* Let $\rho(a) = p_t(a)/p_p(a)$. We partition the vocabulary \mathcal{A} into two sets: $A_C = \{a \mid \rho(a) > C\}$ and
 757 $B_C = \{a \mid \rho(a) \leq C\}$. On any open interval of C where this partition is constant, we can write the KL
 758 divergence $G(C) = -\sum_a p_t(a) \log p_{\text{kept},C}(a)$ as:

$$759 \quad G(C) = -\sum_{a \in A_C} p_t(a) \log \frac{p_p(a)}{Z_C} - \sum_{a \in B_C} p_t(a) \log \frac{p_t(a)/C}{Z_C}$$

760 Differentiating with respect to C (and noting that only Z_C depends on C), we get
 761 $\frac{dG}{dC} = -\frac{d}{dC} \sum_a p_t(a) (-\log Z_C) = \frac{1}{Z_C} \frac{dZ_C}{dC}$. The acceptance rate is $Z_C = \sum_{a \in A_C} p_p(a) + \frac{1}{C} \sum_{a \in B_C} p_t(a)$.
 762 Its derivative is:

$$763 \quad \frac{dZ_C}{dC} = -\frac{1}{C^2} \sum_{a \in B_C} p_t(a).$$

764 Therefore, $G'(C) = \frac{1}{Z_C} \left(-\frac{1}{C^2} \sum_{a \in B_C} p_t(a) \right) \leq 0$, since all terms are non-negative. The derivative is strictly
 765 negative if $\sum_{a \in B_C} p_t(a) > 0$. As $G(C)$ is continuous and piecewise differentiable with a non-positive
 766 derivative, it is non-increasing everywhere. \square

767 **Corollary 1** (Strict Improvement over Proposal). *For any $C > 0$, OBRS produces a distribution $p_{\text{kept},C}$
 768 that is strictly closer to the target distribution p_t than the original proposal distribution p_p , i.e.,*

$$769 \quad \text{KL}(p_t \parallel p_{\text{kept},C}) < \text{KL}(p_t \parallel p_p),$$

770 *unless $p_p = p_t$ or $C \leq \min(\frac{p_t}{p_p})$, in which case the KL divergences are both zero.*

771 *Proof.* From Proposition 1, we know that $\text{KL}(p_t \parallel p_{\text{kept},C})$ is non-increasing in C . In the limit
 772 as $C \rightarrow 0$, the acceptance probability $\alpha_C(a) \rightarrow 1$ for all a , meaning $p_{\text{kept},C} \rightarrow p_p$. Therefore,
 773 $\lim_{C \rightarrow 0} \text{KL}(p_t \parallel p_{\text{kept},C}) = \text{KL}(p_t \parallel p_p)$. For any $C > 0$, as long as $p_p \neq p_t$ and $C > \min(\frac{p_t}{p_p})$, there must
 774 exist some tokens for which $p_t(a) < C \cdot p_p(a)$ or $p_t(a) > C \cdot p_p(a)$, ensuring the condition for a strictly
 775 decreasing KL divergence is met over some interval $(0, C]$. Thus, $G(C) < G(\epsilon)$ for some small $\epsilon > 0$, which
 776 implies $\text{KL}(p_t \parallel p_{\text{kept},C}) < \text{KL}(p_t \parallel p_p)$. \square

777 A.4 PRACTICAL GUIDANCE

- 778 **Setting C .** $C=1$ is a robust default: it contracts the per-prompt KL (strictly unless $p_{\text{inf}}=p_{\text{tr}}$), keeps
 779 acceptance high (Z_1), and is $O(1)$ per token. Larger C pushes q_C closer to p_{tr} but reduces throughput
 $Z_C \leq 1/C$; use it only if variance or bias considerations demand stronger alignment.
- 780 **Compatibility.** The rule uses only per-token log-probabilities already computed by PPO/GRPO, so
 781 it introduces no new estimators and preserves gradient flow exactly as described in Algorithm 1.

782 B DETAILS OF THE EXPERIMENTS

783 B.1 TIS ADJUSTMENT EXPLANATION

784 However, the delay in updates results in staleness, which we magnify for evaluating our method.

785 In this section, we push the above scenario to its limit by asking the inference batch size to be 64x and 128x
 786 the training batch size. Concretely, we choose to use a training batch size of 32. We train models on the
 787 DeepScalerR-Preview dataset Luo et al. (2025), which contains 40k challenging competition math problems.
 788 We select Qwen3-4B-Base and Qwen3-8B-Base models Yang et al. (2025) to run RL on. An important baseline
 789 to our method is the Truncated Importance Sampling (TIS) as in Wu et al. (2025a). However, in the original
 790 technique is proposed only for the approximate models in the inference server. Thus, in the following loss form.

$$802 \quad E_{a \sim \pi(\theta_{\text{old}})} \left[\frac{\pi(\theta_{\text{ref}})}{\pi(\theta_{\text{old,inf}})} \nabla_{\theta} \text{clip} \left(\frac{\pi(\theta_{\text{new}})}{\pi(\theta_{\text{ref}})} \hat{A} \right) \right]$$

803 The weights update frequency is close to on-policy settings, but the gap between the approximate and efficient
 804 inference model and the training weights is the primary goal to solve. However, the original formula cannot
 805 easily be adapted for our extremely large batch setting, as there is no term regularizing the difference between
 806 $\pi_{\theta_{\text{new}}}$ and $\pi_{\theta_{\text{old}}}$. We found that a very simple trick results in a very strong baseline on top of the TIS method,
 807 that is we write it this way.

$$808 \quad E_{a \sim \pi(\theta_{\text{old}})} \left[\frac{\pi(\theta_{\text{new,detached}})}{\pi(\theta_{\text{old,inf}})} \nabla_{\theta} \text{clip} \left(\frac{\pi(\theta_{\text{new}})}{\pi(\theta_{\text{new,detached}})} \hat{A} \right) \right]$$

Table 3: Evaluation scores across benchmarks (GSM8K, MATH-500, AMC22 & AMC23).

Models / Methods	GSM8K		MATH-500		AMC22 & AMC23	
	Mean@4	Pass@4	Mean@4	Pass@4	Mean@4	Pass@4
Qwen3-4B-Base on DeepScaler (rollout batch size = 2048; train batch size = 32; 64 \times)						
On Policy	92.19	95.988	81.55	88.00	58.43	71.76
Off Policy	88.04	95.03	71.15	82.24	39.15	55.57
TIS	89.67	95.53	72.00	80.96	42.77	56.71
TIS with Adjustment	92.76	96.09	79.50	85.81	57.22	66.61
Jackpot (Ours)	92.24	95.891	80.05	85.89	53.916	65.034
Qwen3-4B-Base on DeepScaler (rollout batch size = 4096; train batch size = 32; 128 \times)						
Off Policy	79.70	92.96	60.20	76.60	33.00	48.446
TIS with Adjustment	20.697	43.00	19.10	37.751	7.80	17.83
Jackpot (Ours)	92.00	95.00	80.00	85.50	51.20	60.35
Qwen3-8B-Base on DeepScaler (rollout batch size = 2048; train batch size = 32; 64 \times)						
On Policy	94.238	96.78	93.99	96.65	28.95	37.89
Off Policy	91.05	95.62	77.15	84.90	50.60	65.20
TS with Adjustment	93.85	96.58	82.55	88.38	60.54	72.79
Jackpot (Ours)	94.01	96.63	83.05	88.76	63.55	74.12

where we use the detached most recent model output distribution as the term in the importance sampling. However, the consequence is also very clear, the internal clip around ratio is now 'short-circuited' or no longer useful. Nevertheless, the setting produces very strong convergence is correction over the off-policy baseline. We call it TIS-adjusted.

To fairly compare against the baseline, we also modify our training loss as follows, effectively also 'short-circuiting' the internal ratio clip. The only difference between our setting and theirs is that we use our proposed sampling method to regularize the $\pi_{\theta_{\text{old,inf}}}$.

$$E_{a \sim \pi(\theta_{\text{old}})} \left[\frac{\pi(\theta_{\text{new,detached}})}{\pi(\theta_{\text{old,inf}})^{*new}} \nabla_{\theta} \text{clip} \left(\frac{\pi(\theta_{\text{new}})}{\pi(\theta_{\text{new,detached}})} \hat{A} \right) \right]$$

B.2 FULL DETAILS OF EXTREME SIZE BATCH SIZE EXPERIMENTS

C ABLATION STUDIES ON COMPONENTS OF JACKPOT, THRESHOLD, AND TOP-K

C.1 COMPONENTS' CONTRIBUTION TO JACKPOT

Rejection bridges the gap between the rollout and the current policy (see FP8 on-policy training without explicit jackpot reweighting; this is essentially the vanilla PPO loss with the probability fixed, and the OBRs distribution in this case matches the reference policy exactly). Because the rollout-training distribution gap is now removed, stability is significantly better than the vanilla baseline: even without TIS, training does not crash.

However, without correct importance sampling (see the huge-staleness training regime, where the importance distribution no longer matches P_{ref} but instead matches the current policy), training will eventually collapse.

On the other hand, jackpot reweighting does *not* solve the rollout-training gap (because under the FP8 setting it falls back to vanilla on-policy training, which again leads to a crash). But in the huge-staleness regime, where the rollout-training gap is not the main issue, jackpot reweighting combined with OBRs is effective: it performs correct importance sampling, tracks the proper target distribution, and keeps the overall training procedure stable and efficient.

Table 4: Evaluation scores across benchmarks (AMC12 2024, AIME24, AIME25).

Models / Methods	AMC12 2024		AIME24		AIME25	
	Mean@4	Pass@4	Mean@16	Pass@16	Mean@16	Pass@16
Qwen3-4B-Base on DeepScaler (rollout batch size = 2048; train batch size = 32; 64 \times)						
On Policy	51.11	65.45	23.12	33.13	22.91	30.95
Off Policy	29.44	41.802	13.958	23.03	11.042	18.607
TIS	31.667	50.844	11.875	17.561	11.25	17.278
TIS with Adjustment	43.33	60.67	18.75	26.03	17.708	24.607
Jackpot (Ours)	50.00	63.00	20.625	29.484	18.125	23.627
Qwen3-4B-Base on DeepScaler (rollout batch size = 4096; train batch size = 32; 128 \times)						
Off Policy	24.44	38.41	8.00	15.73	5.00	11.00
TIS with Adjustment	5.00	11.00	1.00	4.00	1.00	2.00
Jackpot (Ours)	47.22	57.99	19.16	24.58	18.52	25.078
Qwen3-8B-Base on DeepScaler (rollout batch size = 2048; train batch size = 32; 64 \times)						
On Policy	54.44	68.47	28.95	37.89	22.50	28.542
Off Policy	40.00	54.75	18.54	28.67	14.16	21.98
TS with Adjustment	48.33	59.78	24.58	35.06	20.00	22.90
Jackpot (Ours)	54.44	66.09	26.87	36.23	20.41	26.57

Table 5: FP8 on-policy training (no staleness). Best scores before crash for the vanilla baseline.

Experiments	AIME24	AMC	MATH500	GSM8K
Vanilla (best before crash)	23.958	57.530	80.900	92.665
Masking-only	25.625	62.048	83.700	92.835
Masking & reweighting	26.667	62.651	82.450	92.305

Table 6: BF16 training with rollout staleness (64/2048). Best scores before crash for masking-only.

Experiments	AIME24	AMC	MATH500	GSM8K
Masking-only (best before crash)	19.167	49.699	78.750	91.793
Masking & reweighting	25.625	63.855	83.800	92.400

C.2 THRESHOLDS, C1, AND C2

Our method involves three hyperparameters: C_1 , C_2 , and the rejection threshold λ . All of them are straightforward to set, and the technique is robust across a wide range of choices.

C_1 . We follow standard truncated importance sampling (TIS) choices. Empirically, selecting $C_1 \in [2, 10]$ consistently works well, and the method is not sensitive within this interval.

C_2 (upper bound for $p_{\theta_{\text{ref}}}/p_{\theta_{\text{new}}}$). This parameter has no practical effect on performance. We set C_2 slightly larger than $1 + \varepsilon_{\text{high}}$ (e.g., 1.28 for DAPO), where any ratio clipped by C_2 would already be clipped by the PPO trust region. Thus, C_2 mainly serves as a conceptual safeguard for ratio stability.

Rejection threshold λ . Our method performs well across all experiments with a default setting of $\lambda = 1.0$, and we recommend choosing λ close to this value. Increasing λ makes the kept-token distribution closer to the target policy but increases the rejection rate. If $\lambda > 1$, it begins rejecting tokens even when the policy and inference distributions are perfectly aligned, causing overly conservative updates. The default value $c = 1.0$ guarantees full acceptance in the matched-distribution case and already reduces KL substantially while keeping a high acceptance rate.

918 **Summary.** Jackpot is stable and easy to configure: C_1 is robust within the typical TIS range 2–10, C_2
 919 has no practical impact once chosen above $1 + \varepsilon_{\text{high}}$, and $c=1.0$ serves as a reliable default.
 920

921 Table 7: Effect of C_1 on benchmark performance. **Experiment Setup:** Model: Qwen3-4B-Base, C2 =
 922 3.0, threshold $c=1.0$, response limit: 8k, mini-batch/train-batch: 64/2048, PPO clip: 0.4/0.7, 100k examples.
 923 Numbers are pass@1 accuracy.

Hyperparameters	AIME24	AMC	MATH500	GSM8K
$C_1=2$	26.875	63.855	82.800	92.267
$C_1=3$	25.625	63.855	83.800	92.703
$C_1=4$	26.042	65.060	83.500	92.684
$C_1=8$	26.875	63.253	83.100	92.437

931 Table 8: Effect of rejection threshold c on benchmark performance. **Experiment Setup:** Model:
 932 Qwen3-4B-Base (target) / Qwen3-1.7B-Base (rollout); Generation length limit: 8K; Training examples:
 933 9K. Numbers are pass@1 accuracy.

Threshold c	AIME24	AMC	MATH500	GSM8K
0.8	14.7	49.4	74.5	92.0
0.9	12.5	47.0	74.6	91.8
1.0	14.7	48.5	74.6	92.2
1.1	12.3	47.4	74.1	92.0
1.2	13.5	45.8	74.1	91.9

C.3 CHOICE OF TOP- K FOR Z APPROXIMATION

In Section 4.4 we approximate the OBRS normalization constant Z by summing over the union of the top- k tokens under p_{inf} and $p_{\theta_{\text{new}}}$, yielding $Z_{\text{approx}} \leq Z$. Increasing k strictly improves this approximation but also increases the number of logits that must be materialized and stored. In the main experiments we therefore fix $k=20$, and here we justify this choice empirically.

We first study the direct effect of k on the quality of the Z estimator. For the extreme off-policy configuration, we log (i) the fraction of the true normalization captured by the top- k estimator, Z_{approx}/Z , and (ii) the calibration factor κ defined in Section 4.4.2, using $k \in \{10, 20, 40\}$. As expected, larger k improves both quantities, but with rapidly diminishing returns. Even for the smallest value $k=10$ we already capture at least 87% of Z at the very beginning of training, and more than 99.98% once the policy has warmed up within few steps; using $k=40$ increases the captured mass only slightly (from roughly 91% initially to about 100.0% in the steady state). Since the union of top-20 tokens is always a superset of the union of top-10 tokens, these diagnostics imply that $k=20$ already yields an almost exact estimator of Z while keeping the additional overhead modest.

We next evaluate how k affects downstream performance. Table 9 reports pass@1 accuracy on our four math benchmarks for Jackpot with $k \in \{10, 20, 40\}$, keeping all other hyperparameters fixed. The differences across choices of k are small and non-monotonic: $k=20$ performs slightly better on AMC and MATH500, while AIME24 and GSM8K show no consistent trend. Overall, the variation is comparable to run-to-run noise, and there is no evidence that pushing k beyond 20 systematically improves task performance. Taken together,

962 Table 9: Effect of top- k on benchmark performance. Numbers are pass@1 accuracy.

Hyperparameters	AIME24	AMC	MATH500	GSM8K
$k=10$	28.958	61.446	82.650	92.608
$k=20$	25.625	63.855	83.800	92.703
$k=40$	27.083	61.446	83.200	92.418

968 these results show that larger k does improve the Z estimator, but the gains become marginal once k reaches
 969 20. Since the computational overhead of our method scales roughly linearly with k , we adopt $k=20$ as
 970 a practical default: it provides an accurate, well-calibrated estimate of Z with negligible additional cost (less
 971 than 3% overhead in our setup), and larger values of k do not yield measurable benefits in our experiments.